Carbohydrate Polymers 89 (2012) 504–510

Carbohydrate Polymers

journal homepage: www.elsevier.com/locate/carbpol

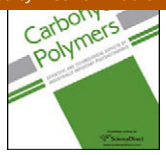

Composites of thermoplastic starch and nanoclays produced by extrusion and thermopressing

Carmen M.O. Müller[a,b], João Borges Laurindo[a], Fabio Yamashita[b,*]

[a] Departamento de Eng. Química e Eng. de Alimentos – Universidade Federal de Santa Catarina, Florianópolis, SC, Brazil
[b] Departamento de Ciência e Tecnologia de Alimentos – Universidade Estadual de Londrina, Londrina, Rod. Celso Garcia Cid (PR 445), Km 380, P.O. Box 6001, CEP 86051-990, Londrina, PR, Brazil

ARTICLE INFO

Article history:
Received 3 November 2011
Received in revised form 15 February 2012
Accepted 13 March 2012
Available online 22 March 2012

Keywords:
Biodegradable film
Biopolymer
Mechanical properties
WVP
TPS

ABSTRACT

The aim of this study was to produce thermoplastic starch (TPS) films and to enhance their properties by reinforcing them with hydrophilic and hydrophobic nanoclays. TPS films were prepared by extrusion and thermopressing, and their crystallinity, water vapor permeability (WVP), and mechanical properties were studied. The hydrophilic nanoclay lowered the material WVP due to the formation of an intercalated composite. The hydrophobic nanoclays increased the rigidity of the films but did not alter the tensile strength. The blending of nanoclays with thermoplastic starch modifies the mechanical properties and WVP, and these changes are strongly associated with the dispersion of nanoclay in the polymer matrix. The dispersion, in turn, depends on the compatibility of the matrix and the nanoclay in terms of the hygroscopicity and the concentration in which the nanoclay is used. The addition of nanoclays to starch-based films is a promising way to enhance them for industrial manufacture.

1. Introduction

The demand for biodegradable materials made from renewable resources is increasing due to the environmental issues concerning conventional synthetic polymers. Starch is a low-cost and abundant biopolymer and there are several studies describing the use of thermoplastic starch (TPS) to produce biodegradable materials such as flexible films and sheets (Yu, Dean, & Li, 2006). To produce the TPS, the granular structure of the starch should be either completely or partially destroyed and transformed into amylose/amylopectin semicrystalline matrix under high temperature and pressure, and using plasticizers (including glycerol, sorbitol, water, and others). The biodegradable films produced with pure TPS have poor mechanical properties and are hygroscopic when compared to those of synthetic polymers due to the hydrophilic nature of the components (Kampeerapappum, Aht-ong, Pentrakoon, & Srikulkit, 2007). Thus, the limited properties of these materials for their usual applications can be improved by the incorporation of other materials (cellulose fibers, nanoclays, or other biodegradable polymers) (Ardakani, Navarchian, & Sadeghi, 2010; Bilck, Grossmann, & Yamashita, 2010; Curvelo, Carvalho, & Agnelli, 2001; Müller, Laurindo, & Yamashita, 2009; Pandey et al., 2005; Park, Lee, Park, Cho, & Ha, 2003; Wilhelm, Seirakowskia, Souzab, & Wypychc, 2003).

Nanocomposites are polymeric materials filled with dispersed particles with at least one dimension in the nanometer range. Common nanofillers include clay, silica nanoparticles, carbon nanotubes, cellulose nanowhiskers and graphene. Among these nanofillers, clays have attracted considerable attention due to their availability, low cost and significant mechanical and barrier enhancement (Chung et al., 2010; Pandey et al., 2005; Rhim, Hong, & Ha, 2009;). Recently, attention has focused on montmorillonite (MMT) minerals to develop nanocomposites (Chaudhary, Miler, Torley, Sopade, & Halley, 2008; Chiou, Yee, Glenn, & Orts, 2005; Cyras, Manfredi, Ton-That, & Vázquez, 2008; Huang, Yu, & Ma, 2006; Kampeerapappum et al., 2007).

However, the modification of nanocomposite properties is associated with the nanoparticles' dispersion in the polymeric matrix; i.e., a good dispersion increases the interfacial area between nanoparticles and polymers, resulting in the properties' improvement (Azeredo, 2009; Chiou et al., 2005; Chung et al., 2010; Weiss, Takhistov, & McClements, 2006). According to the literature, two types of hybrids form in starch/MMT composites: intercalated hybrids and exfoliated hybrids. Intercalation describes the state in which extended polymer chains are present between the clay layers, resulting in a multilayered structure with polymer/inorganic layers at a repeated distance of a few nanometers. Exfoliation describes the state in which the silicate layers are completely

* Corresponding author. Tel.: +55 43 3371 5967; fax: +55 43 3371 4080.
E-mail addresses: fabioy@uel.br, fabioy2@gmail.com (F. Yamashita).

0144-8617 © 2012 Elsevier Ltd. Open access under the Elsevier OA license.
doi:10.1016/j.carbpol.2012.03.035

separated and dispersed in a continuous polymer matrix (Weiss et al., 2006).

According to several authors, nanoclay incorporation in starch-based materials improves the barrier and mechanical properties of composites (Ardakani et al., 2010; Dean, Yu, & Wu, 2007; Huang, Yu, & Ma, 2004; Kampeerapappum et al., 2007; Park et al., 2003). However, these improvements are strongly linked to the clay's nature (hydrophilic or hydrophobic), due to the hydrophilic characteristic of starch.

Park et al. (2003) studied starch/nanoclay composites prepared by casting, employing an organically modified MMT and natural Na^+-MMT. They report that the composites with modified MMT showed higher water vapor transmission rates than samples with Na^+-MMT, as well as inferior mechanical properties. This behavior was associated with modified MMT showing poor dispersion and the presence of large agglomerates, when incorporated into the TPS matrix in comparison to the Na^+-MMT.

Rhim et al. (2009) investigated poly(lactic acid) (PLA)/nanoclay composite films using the casting method and studied the effect of the type of the nanoclay and its concentration on water vapor barrier and mechanical properties. These authors describe that tensile strength, elongation, and water vapor barrier properties of PLA-based composite films vary depending on the type and concentration of nanoclays. They also observe that in composite films without a good clay dispersion of the polymeric matrix, the tensile strength and elongation at break were lower than in PLA pure films.

Several authors report that the use of natural MMT with TPS is an interesting alternative to the production of nanocomposites with starch because, due to their hydrophilic nature, these materials present good dispersion. These composites showed improved thermal stability and better mechanical and barrier (water vapor and gas) properties compared to the samples without nanoclays (Chiou et al., 2005; Huang et al., 2004; Park, Jim, Park, Cho, & Ha, 2002; Park et al., 2003). However, the nanoclay incorporation in TPS materials to produce homogeneous materials with good barrier and mechanical properties remains a challenge (Park et al., 2003; Rhim et al., 2009; Zeppa, Gouanvé, & Espuche, 2009).

The objective of this work is to investigate how different types of nanoclays affect both the crystallinity and the barrier and mechanical properties of TPS composite films obtained by extrusion and thermopressing.

2. Experimental

2.1. Preparation of starch/clay nanocomposite films

The films were prepared with cassava starch (Indemil, Brazil) and glycerol (Dinâmica, Brazil) using 0.25 g of glycerol per gram of starch. Two types of nanoclays at two different concentrations (0.03 and 0.05 g of nanoclay/g of starch, LC and HC, respectively) were used, including one organically modified MMT (Cloisite 30B) and one unmodified MMT (Cloisite Na^+); both were supplied by Southern Clay Products (USA). According to the manufacturer the typical dry particle sizes of both clays are: 10% (v/v) less than 2 μm; 50% (v/v) less that 6 μm and 90% (v/v) less that 13 μm. The starch, glycerol, and nanoclay were mixed in a domestic mixer for 15 min and subsequently extruded, resulting in nanocomposite pellets. The pellets were then thermopressed to obtain the films. The same extruder and thermopressing operation conditions existed for all formulations. A single-screw extruder (BGM, model EL-25, Brazil) with a screw diameter of 25 mm screw diameter (L/D = 30), with 4 heating zones was used for pellet production. The temperature profiles used were 120 °C, 120 °C, 120 °C, and 110 °C, and the screw speed was set at 35 rpm. In the process of thermopressing, 5 g pellets were placed between two sheets of cellulose acetate and the temperature was set at 110 °C. The material was first cast without pressure for 5 min and subsequently pressed at 4 tons for 5 min and then 8 tons for 4 min.

2.2. Scanning electron microscopy (SEM)

Scanning electron microscopy (SEM) of each film sample was performed using a Philips XL-30 scanning electron microscope (Netherlands). The samples were coated with a fine gold layer before the micrographs were obtained.

2.3. Crystallinity

The crystallinity of films and the nanoclay was investigated using XRD. The analysis was performed with a Philips X'Pert diffractometer (Netherlands), using copper radiation Kα ($\lambda = 1.5418$ Å), with a voltage of 40 kV and an operation current of 30 mA. All XRD essays were performed with $2\theta = 2°$ and $2\theta = 70°$ pitch of 0.05°/s.

2.4. Moisture, thickness and density

The films' moisture was determined in triplicate by the gravimetric method, after drying at 105 °C for 24 h, and then expressed in g water/g dry mass. The films' thicknesses were measured using a Digimatic digital micrometer (Mitutoyo Co., Japan) at ten different points of the film. To determine the film density, samples of 20 mm × 20 mm were maintained in a desiccator with phosphorus pentoxide (0% RH) for 20 days (until constant mass) and then weighed. The dry matter densities were then calculated by dividing the mass with the volume.

2.5. Moisture sorption isotherms

Moisture sorption isotherms of the films were determined through the static method, using saturated saline solutions to obtain different relative humidities (Bell and Labuza, 2000). The Guggenheim-Anderson-de Boer (GAB) model was used to represent the experimental equilibrium data, and the model parameters were determined by non-linear regression using Statistica Software 6.0 (Statsoft, USA).

2.6. Water vapor permeability (K^w) and effective water diffusion coefficient (D_w)

The water vapor permeabilities (K^w) of the films were determined gravimetrically at 25 °C, according to the ASTM E 96-00 (2002). Appropriate diffusion cells were used with a permeation area of 0.005 m^2 and with a relative humidity gradient of 2% and 75% RH. The steady state mass transfer in films can be expressed by the mass flux (J) and calculated by Fick's Law (Eq. (1)):

$$J_{wz} = \rho . D_w . \frac{X_1 - X_2}{\delta} \quad (1)$$

where X_1 and X_2 ($X_1 > X_2$) correspond to the moisture in two surfaces of film in g of water/g of the dry solid, ρ is the density of film in g of solid/m^3, D_w is the effective water diffusion coefficient (m^2/s) and δ is the thickness of film in meters. The water mass transfer process depends on the affinity between the water and the polymeric matrix and the resistance to the water molecular movement in its matrix. The moisture content at the film surfaces can be considered as the equilibrium moisture determined from the film water's sorption isotherm.

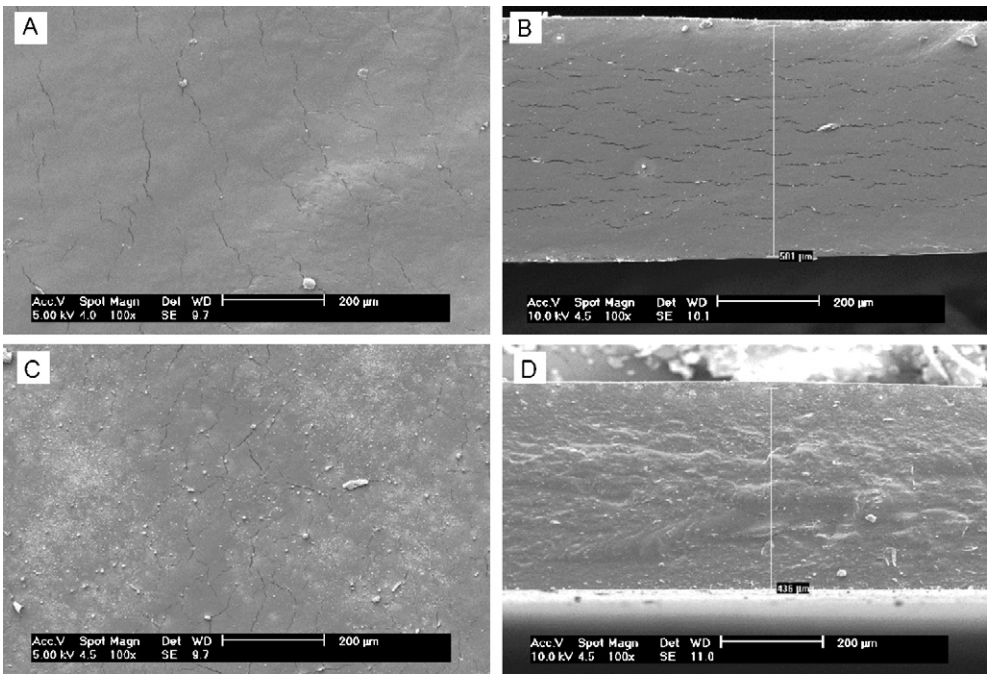

Fig. 1. Micrographs of the composite materials (A, B – Na-LC surface and fracture, respectively; C, D – 30B-HC surface and fracture, respectively).

2.7. Mechanical properties

The mechanical properties of the films were determined from tension tests using the TA-XT2i texture analyzer (England), in accordance with ASTM 882-02 (2002). Samples were clamped between grips and the force and deformation were recorded during extension at 50 mm/min, with an initial distance of 50 mm between the grips. In this way, the tensile strength (MPa), the elasticity modulus (MPa) and the relative deformation at break (%) were determined from ten replicates for each film formulation.

2.8. Dimensional changes during conditioning

The film dimensional change during conditioning was evaluated at two relative humidities: 58% and 75%. For each sample, five specimens (50 mm × 25 mm) were measured at five random points. Subsequently the specimens were conditioned at 25 °C and at a controlled relative humidity. After 8 h and after 240 h the specimens were measured again, and the variation was calculated in relation to the initial length, width, and thickness of each specimen.

3. Results and discussion

3.1. SEM

Fig. 1 shows the micrographs of the surface and the fracture of the samples Na-LC (Fig. 1A and B) and the samples 30B-LC (Fig. 1C and D). In general, the samples with modified nanoclay (30B-LC and 30B-HC) showed more insoluble particles on the films' surface, which may be associated with lower compatibility between the matrix polymer (hydrophilic) and the nanoclay (hydrophobic). This behavior was not observed in samples prepared with the hydrophilic nanoclay (Na-LC and Na-HC), which were uniform and homogeneous without the presence of pores or insoluble particles.

3.2. Crystallinity

Fig. 2 shows the XRD patterns of hydrophilic (Cloisite Na^+) and modified nanoclays (Cloisite B30) and the interlayer spacing of the major peaks. The nanoclay Cloisite 30B showed the principal peak at $2\theta = 4.87°$ corresponding to an interlayer spacing of 18.13 Å. Similar results are reported in the literature about the same nanoclay, showing values between 18.5 and 17.8 Å (Dean et al., 2007; Lee, Chen, & Hanna, 2008; Zeppa et al., 2009). The XRD pattern of Cloisite Na^+ nanoclay showed the principal peak at $2\theta = 7.12°$, which corresponds to 12.41 Å of the interlayer distance (d_{001}).

XRD is a classic method for determining the basal spacing (the d-spacing distance) in clay particles. During melt intercalation, the insertion of the polymer into the organoclay galleries forces the platelets apart and increases the d-spacing, resulting in a shift of the diffraction peak to lower angles (Lee et al., 2008).

Fig. 3 shows the XRD patterns of the films with their interlayer spacing of the principal peaks (d_{001}). The addition of nanoclays in the starch matrix produced more crystalline materials when compared to the control sample. This behavior has been observed by other authors working with hybrid starch and nanoclay

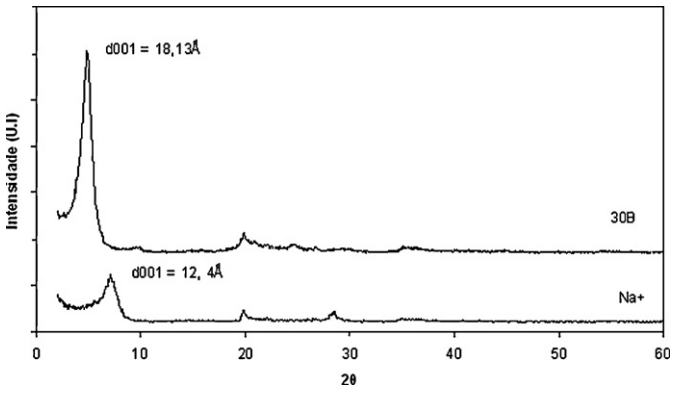

Fig. 2. Diffractogram of Cloisite B30 and Cloisite Na^+ nanoclays.

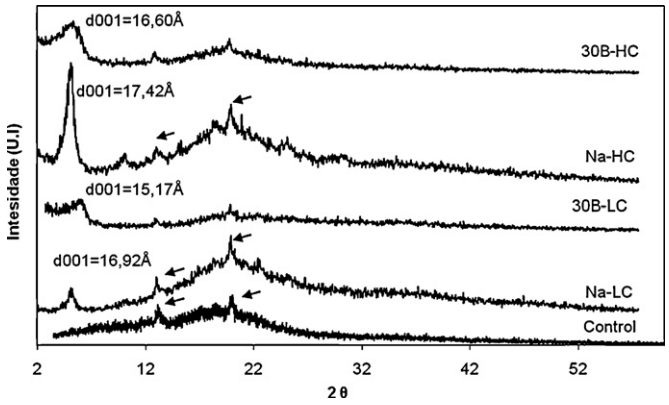

Fig. 3. Diffractogram of films without a nanoclay (Control) and with 3% and 5% of Cloisite 30B (30B-LC and 30B-HC) and Cloisite Na^+ (Na-LC and Na-HC).

composites (Huang et al., 2004; Magalhães and Andrade, 2009; Rhim et al., 2009).

Samples with Cloisite Na^+ showed an increase of interplanar distance (the principal peak) of d_{001} = 12.41 Å in pure nanoclay to 16.92 Å (Na-LC) and 17.42 Å (Na-HC). These results suggest that the starch polymer chains entered into the silicate layers forming intercalate thermoplastic starch-nanoclay composites without complete exfoliation. Several authors associate the increase of interlayer distance with intercalated structural formation in polymers and nanoclay composites (Chivrac, Angellier-Coussy, Guillard, Pollt, & Avérous, 2010; Ma, Yu, & Kennedy, 2005; Park et al., 2003; Tang, Alavi, & Herald, 2008). According to Park et al. (2002), the polar interactions between the hydroxyl groups present in both the starch and the silicate layers probably caused the intercalation of the biopolymer chains into the clay layers' galleries. The starch linear chains (the amylose and parts of the amylopectin) are formed by glucose monomers about 0.55 nm wide (Zhang, Yu, Xie, Naito, & Kagawa, 2007), and the increase of d-spacing in Na-LC and Na-HC composites was 0.45 and 0.50 nm, respectively. We observed that Na-LC and Na-HC samples showed crystalline peaks at Bragg angles of around 13° and 19°. According to Van Soest and Vliegenthart (1997), these peaks correspond to the V_A-type crystallinity of thermoplastic starch. This type of crystallinity is also associated with the amylose recrystallization induced by processing. Other authors report that this type of crystallinity was observed in extruded starch materials with a low moisture content (Hulleman, Kalisvaart, Janssen, Feil, & Vliegenthart, 1999; Rindlav, Hulleman, & Gatenholm, 1997).

Samples 30B-LC and 30B-HC, containing 3% and 5% Cloisite B30, respectively, showed no intercalated compounds because there was no observed increase in intermediate distances compared to the pure nanoclay. This behavior, which was different from the behavior observed for Na-LC and Na-HC, can be associated with a lower nanoclay (hydrophobic) compatibility with the matrix polymer (hydrophilic).

3.3. Thickness, density, and moisture content of the starch nanoclay composite films

Table 1 shows the thickness, density, and moisture content of the films (with and without nanoclays). The materials had similar moisture contents after the thermopressing and ranged from 0.15 ± 0.01 to 0.18 ± 0.02 g water/g dry solid. The moisture content of the films was not affected by the content and nature of the nanoclays.

Table 1
Thickness, density, and moisture content of starch nanoclay composite films.

Film	Moisture (g of water/g of dry solid)	Thickness (μm)	Density (g/cm³)
Control	0.15 ± 0.01[a]	394 ± 28[a]	1.23 ± 0.17[a]
Na-LC	0.18 ± 0.02[a]	485 ± 37[b]	1.34 ± 0.04[a]
30B-LC	0.16 ± 0.01[a]	466 ± 25[a,b]	1.24 ± 0.12[a]
Na-HC	0.15 ± 0.01[a]	515 ± 37[b]	1.42 ± 0.05[a]
30B-HC	0.15 ± 0.01[a]	447 ± 35[a,b]	1.36 ± 0.03[a]

Different lower case letters (a,b) at the same column indicate significant differences between samples (Tukey test at $p \leq 0.05$).

The composites with hydrophilic nanoclays tended to be thicker than the materials without nanoclays (Control) but there was no significant difference between the composites' thicknesses.

There was no significant difference among the densities of the films with and without nanoclays or with the nanoclay concentration. The density values were similar to those reported by Chivrac et al. (2010) for wheat starch and nanoclay films that had values between 1.46 ± 0.06 and 1.51 ± 0.05 g/cm³.

3.4. Moisture sorption isotherm

All samples presented sigmoid sorption isotherms (Type II), which characterize the hydrophilic nature of the films—even those with nanoclays. The water activity from 0.6 and 0.9 caused an increase in moisture for all films, and this behavior is associated with a "water clustering" phenomenon (Godbillot, Dole, Joly, Rogé, & Mathlouthi, 2006; Müller et al., 2009; Peng, Chen, Wu, & Jiang, 2007; Zeppa et al., 2009).

Samples containing nanoclays showed similar equilibrium moisture content, indicating that the nanoclay nature and concentration did not significantly alter the moisture sorption properties of composites. The moisture equilibrium values were in accordance with those reported by others who studied starch/nanoclay composites (Chivrac et al., 2010; Enrione, Hill, & Mitchell, 2007).

The control sample showed an equilibrium moisture content similar to the composite samples, and these results were in accordance with those reported by Chivrac et al. (2010), who worked with wheat starch and MMT. They did not observe a significant difference in equilibrium moisture values between films with and without clay.

Cyras et al. (2008), working with composites of MMT and potato starch prepared by casting, determined the moisture sorption at 75% RH, and they obtained similar results when comparing films without nanoclays and with 5% MMT. We would like to emphasize that there are few reports in the literature concerning the water sorption behavior of cassava thermoplastic starch and nanoclay composites.

The parameters (m_0, C, k) of the GAB model are shown in Table 2. The GAB model adjusted satisfactorily to the experimental data, as already shown by other authors who have worked with biofilms based on starch (Enrione et al., 2007; Godbillot et al., 2006; Mali,

Table 2
GAB model parameters for moisture sorption isotherms for the starch (Control) and composite films (Na-LC, 30B-LC, Na-HC, 30B-HC).

Film	GAB model parameter		
	m_0	k	C
Control	0.07	0.95	5.65
Na-LC	0.10	0.90	2.68
30B-LC	0.07	0.97	11.00
Na-HC	0.07	0.97	7.86
30B-HC	0.08	0.93	5.58

m_0 in g of water/g of dry solid. The coefficient of determination (R^2) > 0.99 for all fitted models.

Table 3
Water vapor permeability (K^w), moisture content at the film surface (X_1 and X_2), mass flux (J) and effective diffusion coefficient (D_w) of the starch film (Control) and starch and nanoclay composites (Na-LC, 30B-LC, Na-HC and 30B-HC).

Film	K^w ($\times 10^7$) (g water/h m Pa)	X_1 (a_w = 0.75) (g water/g dry solid)	X_2 (a_w = 0.02) (g water/g dry solid)	J (g water/m^2 h)	D_w ($\times 10^{12}$) (m^2/s)
Control	7.83 ± 0.71	0.2482	0.0077	4.59	1.70
Na-LC	2.91 ± 0.89	0.2533	0.0046	1.39	0.56
30B-LC	6.77 ± 0.67	0.2312	0.0120	3.36	1.60
Na-HC	2.91 ± 0.63	0.2343	0.0092	1.31	0.59
30B-HC	5.43 ± 0.39	0.2437	0.0077	2.81	1.09

Sakanaka, Yamashita, & Grossmann, 2005; Müller, Yamashita, & Laurindo, 2008).

The parameter m_0 is associated both with the water content of the monolayer, and films without nanoclay (Control) showed m_0 values similar to the values reported by other authors who studied starch films (Krochta and Sothornvit, 2001; Mali et al., 2005; Müller et al., 2008; Zeppa et al., 2009). The m_0 values of the control films are consistent with those reported by Enrione et al. (2007) for thermoplastic starch that related values between 0.056 and 0.094 g water/g dry solid. The monolayer content was not affected by the concentration and hydrophilic nature of the nanoclay; this is because the sorption mechanism is governed mainly by the polymer matrix. According to Masclaux, Gouanvé, and Espuche (2010), for starch-based films reinforced with MMT and independent of the nanoclay charge, the water sorption isotherms are similar to the reference matrix. These authors worked with potato-starch/nanoclay composites, and they observed differences in sorption curves only with 7.5% MMT composites; they attribute this behavior to two antagonistic mechanisms. The matrix and nanoclay sorption sites contribute to the total moisture content in separate ways when they are not interacting among themselves. With higher nanoclay concentrations, the behavior of the matrix changes due to geometric constraints such as changes in mobility of the polymer chain.

Parameter C is classically associated with the heat of sorption of the monolayer and showed similar behavior in all samples. The C values are consistent with values reported by other researchers who worked with hydrophilic biofilms (Brandelero, Grossmann, & Yamashita, 2011; Mali et al., 2005; Müller et al., 2009).

3.5. Water vapor permeability, mass flux and diffusion

Table 3 presents the water vapor permeability of the films using a relative humidity gradient of ΔRH = 2–75%, the moisture content at the film surface (X_1 and X_2), the water mass flux (J), and the effective diffusion coefficient (D_w).

Composite samples showed a lower water mass flow than samples without nanoclays, which was caused by the lower diffusivities that these materials presented. The lower effective diffusion coefficient of samples containing nanoclays was reported by other authors, and was associated with the increased tortuosity of the system due to the clay (Cyras et al., 2008; Huang et al., 2004; Park et al., 2003). According to Weiss et al. (2006), the lamellae are distributed in nanocomposites in the polymer matrix, forcing the vapor to flow through a tortuous path and thus forming a complex barrier system. The higher the tortuosity of the system, the better the material barrier properties.

The Na-LC and Na-HC films showed the lowest water vapor permeability and effective diffusion coefficient, which was probably due to the better compatibility between the Cloisite Na$^+$ nanoclay and the polymer matrix. This behavior corroborates the crystallinity results of these samples where there was a significant increase in the interlayer distance, indicative of the formation of intercalated composites.

3.6. Mechanical properties

Table 4 shows the results of mechanical tests in terms of tensile strength (T), elongation at break (ε) and Young's modulus (Y).

The addition of nanoclays did not significantly modify the elongation at the break of the composites because the layered silicates probably provided some new nucleation sites and thus contributed to the crystallites' growth (Cyras et al., 2008; Magalhães and Andrade, 2009). Moreover, the composites that used the nanoclay Cloisite Na$^+$ (Na-LC and Na-HC) were more rigid (had a higher Young's modulus) due to the intercalated structures. According to Ardakani et al. (2010), the greater gallery spacing represents more starch molecules diffused into the space between the silicate layers and thus, higher interfacial interactions that lead to more intensive reinforcing effects.

3.7. Dimensional changes of the films conditioned at different relative humidities

Some specimens for mechanical testing were previously conditioned at a specific relative humidity; changes were noticed in their dimensions, and this behavior was also reported by both Brandelero et al. (2011) for extruded cassava starch and poly (butylen adipate co-terephthalate) films and by Thunwall, Kuthanová, Boldizar, and Rigdahl (2008) for extruded potato-starch films. Both researchers associated this phenomenon with a more compact conformation of starch due to the extrusion process that could guide the polymer chains.

All films showed a thickness increase after conditioning time and, as observed in width, this dimensional change was higher in samples conditioned at 75% RH (Fig. 4). The films became thicker with conditioning time for both the RHs evaluated.

For all films, there was a decrease in the length after conditioning time but there was no correlation with the conditioning time or the RH (Fig. 4).

All films showed a decrease in width during conditioning, and for the specimens conditioned at higher relative humidity (RH = 75%) this effect was greater; there was also a positive correlation between conditioning time and shortening (Fig. 4).

As all films showed changes in their dimensions after conditioning times at different RH; there is probably a correlation between these changes and the sorption properties, and more detailed studies of this phenomenon should be performed.

Table 4
Mechanical properties of starch and nanoclay composite films.

Film	T (MPa)	ε (%)	Y (MPa)
Control	0.96 ± 0.13	63 ± 12	16 ± 4
Na-LC	0.88 ± 0.13	76 ± 12	90 ± 1
30B-LC	1.57 ± 0.19	75 ± 13	20 ± 1
Na-HC	2.22 ± 0.18	76 ± 8	50 ± 8
30B-HC	1.51 ± 0.12	74 ± 5	20 ± 5

T: tensile strength; ε: elongation at break; Y: Young's modulus.

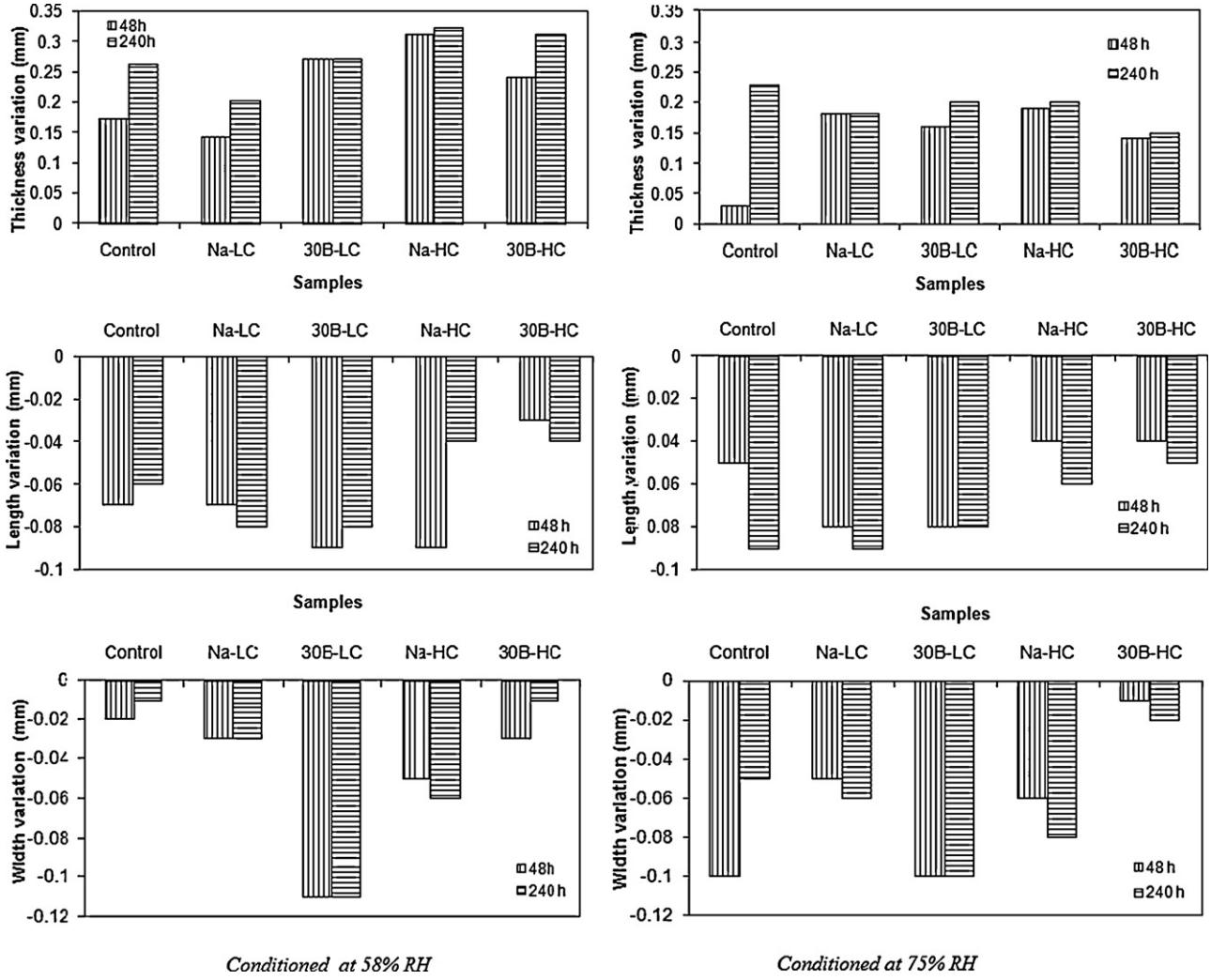

Fig. 4. Width, thickness and length variations of starch and starch/nanoclay films conditioned at 58% and 75% RH for 48 and 240 h.

4. Conclusion

The blending of nanoclays with thermoplastic starch modifies the mechanical properties and barrier to water vapor, and these changes are strongly associated with the dispersion of nanoclay in the polymer matrix. The dispersion, in turn, depends on the compatibility of the matrix and the nanoclay in terms of the hygroscopicity and the concentration in which the nanoclay is used. For materials consisting of starch, the use of 5% hygroscopic nanoclay increases strength and decreases the permeability to water vapor. In addition, due to the ease of the incorporation of nanoclay into the TPS films, the addition of nanoclays to starch-based films is a promising way to enhance them for industrial manufacture.

Acknowledgments

The authors would like to acknowledge the financial support of CNPq and CAPES.

References

Ardakani, K. M., Navarchian, A. H., & Sadeghi, F. (2010). Optimization of mechanical properties of thermoplastics starch/clay nanocomposites. *Carbohydrate Polymers*, *79*, 547–554.

ASTM 882-02. (2002). *Standard test methods for tensile properties of thin plastic sheeting*.

ASTM E 96-00. (2002). *Standard test methods for water vapor transmission of materials*.

Azeredo, H. M. D. (2009). Nanocomposites for food packaging applications. *Food Research International*, *42*, 1240–1253.

Bell, L. N., & Labuza, T. P. (2000). *Moisture sorption: Practical aspects of isotherm measurement and use*. Egan, USA: AACC Egan Press.

Bilck, A. P., Grossmann, M. V. E., & Yamashita, F. (2010). Biodegradable mulch films for strawberry production. *Polymer Testing*, *29*, 471–476.

Brandelero, R. P. H., Grossmann, M. V. E., & Yamashita, F. (2011). Effect of the method of production of the blends on mechanical and structural properties of biodegradable starch films produced by blown extrusion. *Carbohydrate Polymers*, *86*, 1344–1350.

Chaudhary, A. L., Miler, M., Torley, P. J., Sopade, P. A., & Halley, P. J. (2008). Amylose content and chemical modification effects on the extrusion of thermoplastic starch from maize. *Carbohydrate Polymers*, *74*, 907–913.

Chiou, B. S., Yee, E., Glenn, G. M., & Orts, W. J. (2005). Rheology of starch–clay nanocomposites. *Carbohydrate Polymers*, *59*, 467–475.

Chivrac, F., Angellier-Coussy, H., Guillard, V., Pollt, E., & Avérous, L. (2010). How does water diffuse in starch/montmorillonite nano-biocomposite materials? *Carbohydrate Polymers*, *82*, 128–135.

Chung, Y. L., Ansari, S., Estevez, L., Hayrapetyan, S., Giannelis, E. G., & Lai, H. M. (2010). Preparation and properties of biodegradable starch–clay nanocomposites. *Carbohydrate Polymers*, *79*, 391–396.

Curvelo, A. A. S., Carvalho, A. J. F., & Agnelli, J. A. M. (2001). Thermoplastic starch-cellulosic fibers composites: Preliminaries results. *Carbohydrate Polymer*, *45*, 183–188.

Cyras, V. P., Manfredi, L. B., Ton-That, M. T., & Vázquez, A. (2008). Physical and mechanical properties of thermoplastic starch/montmorillonite nanocomposite films. *Carbohydrate Polymers*, *73*, 55–63.

Dean, K., Yu, L., & Wu, D. L. (2007). Preparation and characterization of melt-extruded thermoplastic starch/clay nanocomposites. *Composites Science and Technology*, *67*, 413–421.

Enrione, J. I., Hill, S. E., & Mitchell, J. R. (2007). Sorption and diffusional studies of extruded waxy maize starch-glycerol systems. *Starch/Stärke*, *59*, 1–9.
Godbillot, L., Dole, P., Joly, C., Rogé, B., & Mathlouthi, M. (2006). Analysis of water binding in starch plasticized films. *Food Chemistry*, *96*, 380–386.
Huang, M., Yu, J., & Ma, X. (2004). Studies on the properties of montmorillonite-reinforced thermoplastic starch composites. *Polymer*, *45*, 7017–7023.
Huang, M., Yu, J., & Ma, X. (2006). High mechanical performance MMT-urea and formamide-plasticized thermoplastic cornstarch biodegradable nanocomposites. *Carbohydrate Polymers*, *63*, 393–399.
Hulleman, S. H. D., Kalisvaart, M. G., Janssen, F. H. P., Feil, H., & Vliegenthart, J. F. G. (1999). Origins of B-type crystallinity in glycerol-plasticized, compression moulded potato starches. *Carbohydrate Polymers*, *39*, 351–360.
Kampeerapappum, P., Aht-ong, D., Pentrakoon, D., & Srikulkit, K. (2007). Preparation of cassava starch: Montmorillonite composite films. *Carbohydrate Polymers*, *67*, 155–163.
Krochta, J. M., & Sothornvit, R. (2001). Plasticizer effect on mechanical properties of β-lactoglobulin films. *Journal of Food Engineering*, *50*, 149–155.
Lee, S. Y., Chen, H., & Hanna, M. A. (2008). Preparation and characterization of tapioca starch–poly(lactic acid) nanocomposite foams by melt intercalation based on clay type. *Industrial Crops and Products*, *28*, 95–106.
Ma, X., Yu, J., & Kennedy, J. F. (2005). Studies on the properties of natural fibers-reinforced thermoplastic starch composites. *Carbohydrate Polymer*, *62*, 19–24.
Magalhães, N. F., & Andrade, C. T. (2009). Thermoplastic corn starch/clay hybrids: Effect of clay type and content on physical properties. *Carbohydrate Polymers*, *75*, 712–718.
Mali, S., Sakanaka, L. S., Yamashita, F., & Grossmann, M. V. E. (2005). Water sorption and mechanical properties of cassava starch films and their relation to plasticizing effect. *Carbohydrate Polymers*, *60*, 283–289.
Masclaux, C., Gouanvé, F., & Espuche, E. (2010). Experimental and modelling studies of transport in starch nanocomposite films as affected by relative humidity. *Journal of Membrane Science*, *363*, 221–231.
Müller, C. M. O., Laurindo, J. B., & Yamashita, F. (2009). Effect of cellulose fibers addition on the mechanical properties and water vapor barrier of starch based films. *Food Hydrocolloids*, *23*, 1328–1333.
Müller, C. M. O., Yamashita, F., & Laurindo, J. B. (2008). Evaluation of the effects of glycerol and sorbitol concentration and water activity on the water barrier properties of cassava starch films through a solubility approach. *Carbohydrate Polymers*, *72*, 82–87.
Pandey, J. K., Kumar, A. P., Misra, M., Mohanty, A. K., Drzal, L. T., & Singh, R. P. (2005). Recent advances in biodegradable nanocomposites. *Journal of Nanoscience and Nanotechnology*, *5*, 497–526.
Park, H. W., Jim, C. Z., Park, C. Y., Cho, W. J., & Ha, C. S. (2002). Preparation and properties of biodegradable thermoplastic starch/clay hybrids. *Macromolecular Materials and Engineering*, *287*, 553–558.
Park, H. W., Lee, W. K., Park, C. Y., Cho, W. J., & Ha, C. S. (2003). Environmentally friendly polymer hybrids. Part I. Mechanical, thermal and barrier properties of thermoplastics starch/clay nanocomposites. *Journal of Material Science*, *38*, 909–915.
Peng, G., Chen, X., Wu, W., & Jiang, X. (2007). Modeling of water sorption isotherm for corn starch. *Journal of Food Engineering*, *80*, 562–567.
Rhim, J. W., Hong, S. I., & Ha, C. S. (2009). Tensile, water vapor barrier and antimicrobial properties of PLA/nanoclay composite films. *LWT – Food Science and Technology*, *42*, 612–617.
Rindlav, A., Hulleman, S. H. D., & Gatenholm, P. (1997). Formation of starch films with varying crystallinity. *Carbohydrate Polymer*, *34*, 25–30.
Tang, X., Alavi, S., & Herald, T. J. (2008). Effects of plasticizers on the structure and properties of starch–clay nanocomposite films. *Carbohydrate Polymers*, *74*, 552–558.
Thunwall, M., Kuthanová, V., Boldizar, A., & Rigdahl, M. (2008). Film blowing of thermoplastic starch. *Carbohydrate Polymers*, *71*, 583–590.
Van Soest, J. J. G., & Vliegenthart, J. F. G. (1997). Crystallinity in starch plastics: Consequence for material properties. *Trends in Biotechnology*, *15*, 208–213.
Weiss, J., Takhistov, P., & McClements, J. (2006). Functional materials in food nanotechnology. *Journal of Food Science*, *71*, 107–116.
Wilhelm, H. M., Seirakowskia, M. R., Souzab, G. P., & Wypychc, F. (2003). Starch films reinforced with mineral clay. *Carbohydrate Polymer*, *52*, 101–110.
Yu, L., Dean, K., & Li, L. (2006). Polymer blends and composites from renewable resources. *Progress in Polymer Science*, *31*, 576–602.
Zeppa, C., Gouanvé, F., & Espuche, E. (2009). Effect of a plasticizer on structure of biodegradable starch/clay nanocomposites: Thermal, water-sorption and oxygen-barrier properties. *Journal of Applied Polymer Science*, *112*, 2044–2056.
Zhang, Q. X., Yu, Z. Z., Xie, X. L., Naito, K., & Kagawa, Y. (2007). Preparation and crystalline morphology of biodegradable starch/clay nanocomposites. *Polymer*, *48*, 7193–7200.